12 Renal Sinus Neoplasms

Sung Eun Rha and Jae Young Byun

CONTENTS

12.1 Introduction

The renal sinus is the medial compartment of the kidney that surrounds the kidney's pelvocalyceal system and communicates with the perinephric space (Figs. 12.1, 12.2). The major branches of the renal artery and vein along with the major and minor calyces of the collecting system are located within the renal sinus. The remainder of the sinus is filled with adipose tissue, lymphatic channels, nerve fibers of the autonomic nervous system, and varying quantities of fibrous tissue (Amis 2000; Amis and Cronan 1988; Davidson et al. 1999; Zagoria and Tung 1997b). Of these constituents, fat is the largest single component of the renal sinus and is readily seen with ultrasound (US), computed tomography (CT), and magnetic resonance (MR) imaging. The quantity of fat in the renal sinus normally and gradually increases with age and obesity (Fig. 12.3; Zagoria and Tung 1997b). Observation of renal sinus fat is important for detecting small tumors in that area, as well as for determining the exact tumor staging.

Renal sinus involvement of tumors is significant because the renal sinus contains numerous lymphatics and veins that may permit dissemination of a tumor otherwise regarded as renal limited. Because there is no fibrous capsule separating the renal cortex of the columns of Bertin from the renal sinus fat, a renal tumor may continue unrestricted into the sinus fat, which is rich in veins and lymphatics (Bonsib et al. 2000). Although renal sinus involvement is not currently used in either the Robson or TNM staging systems, the centrally located renal

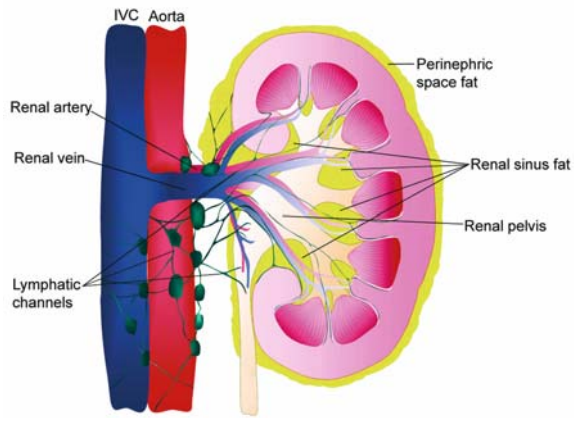

Fig. 12.1. Diagrammatic illustration shows the normal anatomy and major constituents of the renal sinus. Note that fat is the largest component of the renal sinus. (With permission from Rha et al. 2004)

S. E. Rha, MD
Assistant Professor, Department of Radiology, Kangnam St. Mary's Hospital, College of Medicine, The Catholic University of Korea, 505 Banpo-Dong, Seocho-Ku, Seoul 137-040, South Korea
J. Y. Byun, MD
Professor and Chairman, Department of Radiology, Kangnam St. Mary's Hospital, College of Medicine, The Catholic University of Korea, 505 Banpo-Dong, Seocho-Ku, Seoul 137-040, South Korea

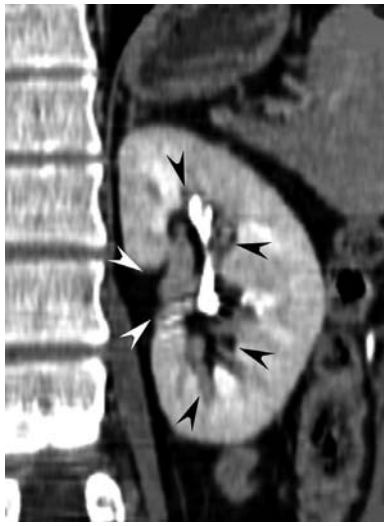

Fig. 12.2. Normal CT anatomy of the renal sinus in a 57-year-old man. Coronal contrast-enhanced CT scan obtained during the excretory phase clearly shows the extent of the renal sinus (*arrowheads*). (With permission from Rha et al. 2004)

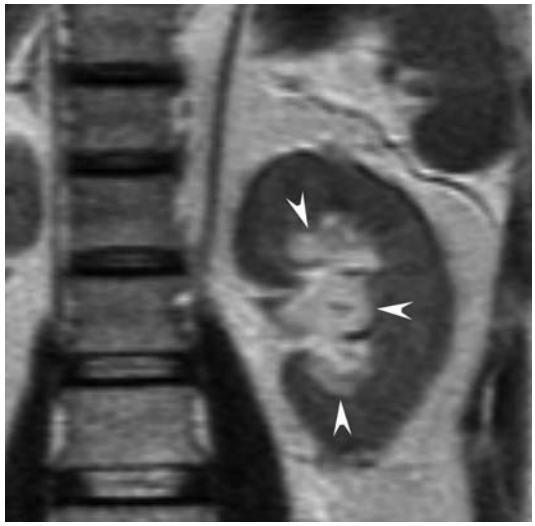

Fig. 12.3. Magnetic resonance imaging anatomy of renal sinus in a 73-year-old man with renal sinus lipomatosis. Coronal turbo spin-echo T2-weighted MR image (TR=6500 ms, TE=120 ms) shows prominent fat in the left renal sinus (*arrowheads*).

tumors in the renal sinus may affect surgical planning and prognosis of the renal tumors.

A broad spectrum of benign and malignant neoplasms exist involving the renal sinus, either arising primarily from sinus structures or secondarily extending into the sinus from the adjacent cortex or retroperitoneum. Tumors involving the renal sinus can be classified depending on their origins into four subgroups: (a) epithelial tumors of the renal pelvis; (b) mesenchymal tumors of the renal sinus; (c) renal parenchymal tumors projecting into the renal sinus; and (d) retroperitoneal tumors extending to the renal sinus.

12.2 Imaging Modalities for Renal Sinus Tumors

Various imaging modalities can be used for the evaluation of tumors affecting the renal sinus; these include excretory urography, US, CT, MR imaging, and angiography. Each modality can provide useful information regarding the detection, characterization, and extent of tumors.

Excretory urography is useful for evaluating the involvement of the renal collecting system. Most neoplastic conditions of the renal sinus are focal and are termed parapelvic (the prefix "para" means "alongside" or "beside"). These abnormalities cause focal displacement and compression of the pelvocalyceal system on excretory urography and a circumscribed mass on cross-sectional images. Irregular pelvocalyceal deformity suggests direct invasion by malignant tumors or unusual inflammatory conditions. A very large tumor displaces the kidney laterally and may cause anterior rotation. Conversely, disorders that diffusely surround the pelvocalyceal system are termed peripelvic (the prefix "peri" means "around"). The representative peripelvic neoplastic condition is renal lymphoma infiltrating the renal sinus, which causes generalized effacement and stretching of the pelvocalyceal system on excretory urography, mimicking renal sinus lipomatosis or renal sinus cyst (Davidson et al. 1999).

Ultrasound functions as the initial screening modality for noninvasive imaging of the kidney and is useful in distinguishing cystic from solid space-occupying tumors when excretory urography detects the lesions. Normal renal sinus is imaged as an area of increased echo with variable contours due to the fat–parenchyma interface (Fig. 12.4). A collapsed renal pelvis may be indistinguishable from echogenic renal sinus fat. Despite good results with US, there are limitations, especially with small lesions when the renal sinus lesion is poorly defined or the echo pattern is similar to or the same as the adjacent renal sinus fat or adjacent renal parenchyma (Rosenfield et al. 1979).

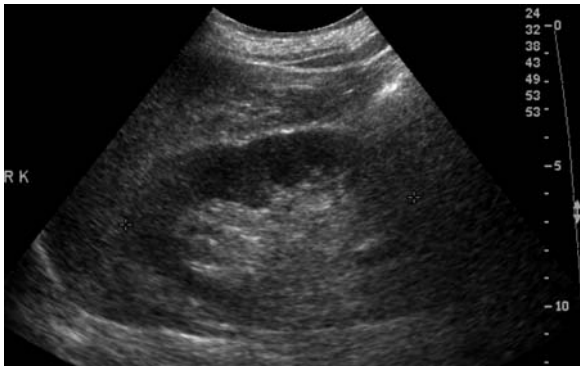

Fig. 12.4. Normal US anatomy of the renal sinus in a 73-year-old man with renal sinus lipomatosis. Longitudinal US image of right kidney shows prominent renal sinus as a central hyperechoic area with variable contours due to the fat–parenchyma interface.

Computed tomography is the most sensitive, efficient, and comprehensive imaging modality for evaluating the kidneys and is the problem-solving technique for a wide variety of renal sinus tumors. The recent development of multidetector CT provides dramatically increased speed of scan acquisition and improved spatial resolution through the use of thinner collimation. Multiplanar reconstruction images can allow exact determination of the extent of complex renal sinus tumors (Jeffrey 2004). In general, the coronal plane is the most useful for the evaluation of renal sinus lesions because it provides a comprehensive view of the kidney including the renal sinus (Pozzi-Mucelli et al. 2004).

Magnetic resonance imaging is an alternative to CT for the evaluation of renal sinus tumors as it allows detailed tissue characterization of complicated renal sinus tumors and direct multiplanar images with the same image resolution in the coronal, sagittal, and axial planes, and it can also be used in patients with renal failure or contrast material allergies (Pozzi-Mucelli et al. 2004).

12.3 Epithelial Tumors of the Renal Pelvis

Malignant tumors arising from the urothelium of the renal pelvis constitute only 5% of urinary tract neoplasms. Approximately 90% of pelvocalyceal cancers are transitional cell carcinomas and the remaining 10% are squamous cell carcinomas. These tumors are centered in the renal pelvis and secondarily invade the renal sinus fat and renal parenchyma (Pickhardt et al. 2000).

12.3.1 Transitional Cell Carcinoma

Transitional cell carcinoma of the renal pelvis is epidemiologically similar to that of the bladder: there is male predominance; typical patient age at diagnosis is the sixth or seventh decade of life; and tobacco and industrial carcinogens are risk factors (McLaughlin et al. 1983). Hematuria is the principal symptom and multifocality is a significant problem for patients with transitional cell carcinomas in the upper urinary tract. Nearly 50% of patients have a history of urothelial carcinoma of the bladder or ureters or later develop urothelial carcinoma.

Depending on the gross morphologic features, transitional cell carcinomas are classified into papillary, infiltrating, and mixed papillary and infiltrating. Eighty-five percent of renal pelvis transitional cell carcinomas are papillary. Papillary transitional cell carcinomas are characterized by their frondlike morphologic structure, with the fronds lined by a thick layer of transitional epithelium. Infiltrating tumors are characterized by thickening and induration of the renal pelvic wall. If the renal pelvis is involved, there is often invasion into the renal parenchyma (Wong-You-Cheong et al. 1998). Pathologically, stage I transitional cell carcinomas of the renal pelvis are limited to the uroepithelium and lamina propria mucosae. Stage II tumors invade to, but not beyond, the muscularis. Stage III tumors infiltrate into the renal parenchyma or the peripelvic fat. Stage IV tumor is defined by local extrarenal extension, lymph node involvement, or distant metastasis (Wong-You-Cheong et al. 1998).

On excretory urography, transitional cell carcinomas of the renal pelvis may show imaging findings such as intraluminal filling defects due to tumor or blood, amputated calyces resulting from malignant stricture, hydronephrosis caused by tumor obstruction of the ureteropelvic junction, or nonfunctioning kidney. Ultrasound shows a poorly defined soft tissue mass replacing the renal sinus fat (Fig. 12.5; Wong-You-Cheong et al. 1998).

Typical CT findings include a sessile or flat solid mass in the renal calyces and/or pelvis, or focal renal pelvic wall thickening or infiltrating mass (Baron et al. 1982). Obstruction occurs earlier or later in the natural history of a given tumor

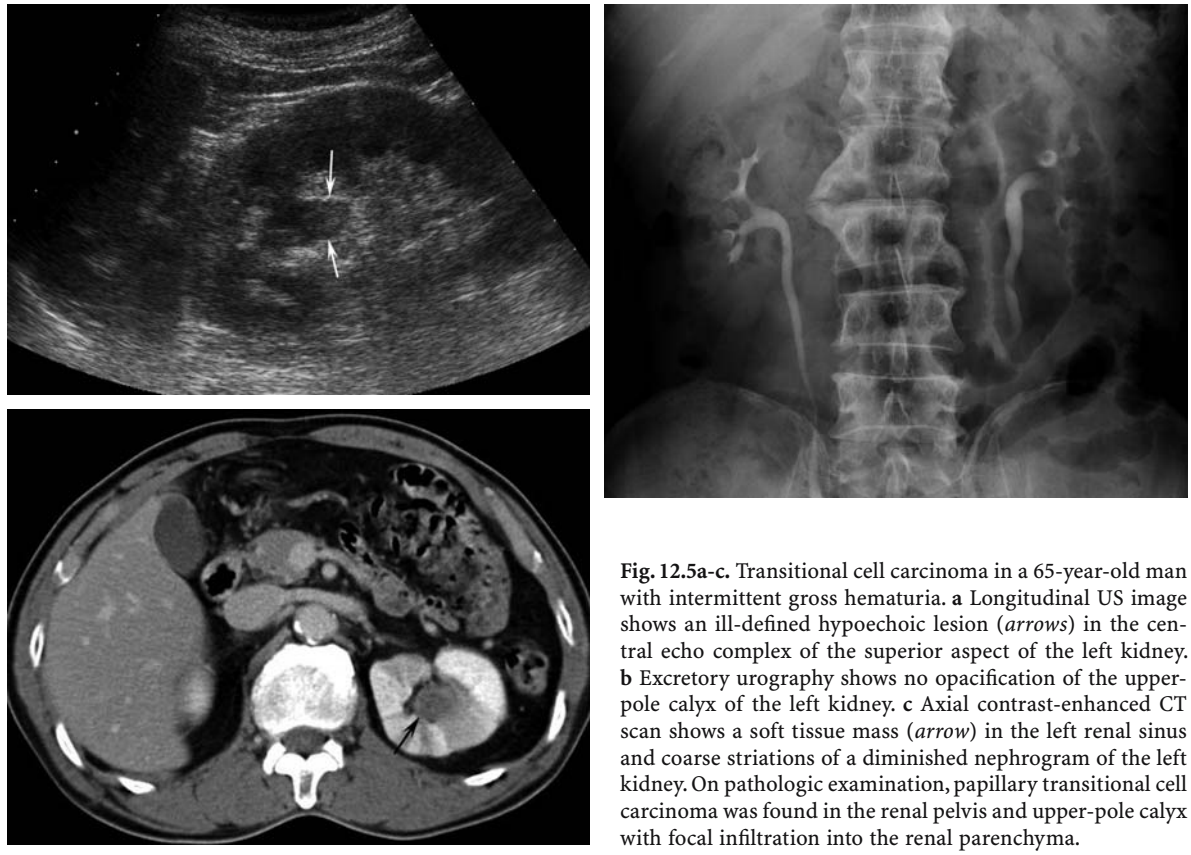

Fig. 12.5a-c. Transitional cell carcinoma in a 65-year-old man with intermittent gross hematuria. **a** Longitudinal US image shows an ill-defined hypoechoic lesion (*arrows*) in the central echo complex of the superior aspect of the left kidney. **b** Excretory urography shows no opacification of the upper-pole calyx of the left kidney. **c** Axial contrast-enhanced CT scan shows a soft tissue mass (*arrow*) in the left renal sinus and coarse striations of a diminished nephrogram of the left kidney. On pathologic examination, papillary transitional cell carcinoma was found in the renal pelvis and upper-pole calyx with focal infiltration into the renal parenchyma.

depending on its anatomic location and pattern of growth. On CT and MR imaging, early-stage transitional cell carcinoma of the kidney, stage I or II, is a central solid mass in the renal pelvis that expands centrifugally with compression of the renal sinus fat and appears separated from the renal parenchyma either by renal sinus fat or excreted contrast material (Fig. 12.6); however, CT has limited ability to differentiate between stage I and stage II carcinomas (Urban et al. 1997a). On the contrary, invasive transitional cell carcinoma, stage III or IV, obliterates the renal sinus fat and infiltrates into the surrounding parenchyma, typically not disturbing its reniform contour (Fig. 12.7, 12.8; Urban et al. 1997b). This growth pattern is helpful for differentiating transitional cell carcinoma from renal cell carcinoma, which tends to grow by expansion. Differentiation from renal cell carcinoma is usually suggested when CT reveals the relatively central location of the tumor, its centrifugal expansion or invasion of the kidney, its hypovascular nature, or a combination of these findings (Kawashima and Goldman 2000).

12.3.2 Squamous Cell Carcinoma

Approximately 10% of renal pelvic tumors are squamous cell carcinomas. Squamous cell carcinomas are strongly associated with renal calculi, and chronic irritation of the urothelium appears to be an important etiologic factor in the development of squamous cell carcinoma (Blacher et al. 1985). Imaging findings of squamous cell carcinomas are indistinguishable from those of transitional cell carcinomas (Fig. 12.9); however, when compared with the transitional cell carcinomas, squamous cell carcinoma of the kidney tends to appear with predominantly extraluminal tumor extension rather than purely intraluminal tumor growth on CT (Narumi et al. 1989). The presence of a renal stone in association with a geographic infiltrating renal lesion with a large renal sinus component implies the diagnosis of squamous cell carcinoma (Fig. 12.10; Wimbish et al. 1983). Most squamous cell carcinomas of the renal pelvis are high stage. Extensive infiltration of the renal parenchyma is common and survival for 5 years is rare (Blacher et al. 1985).

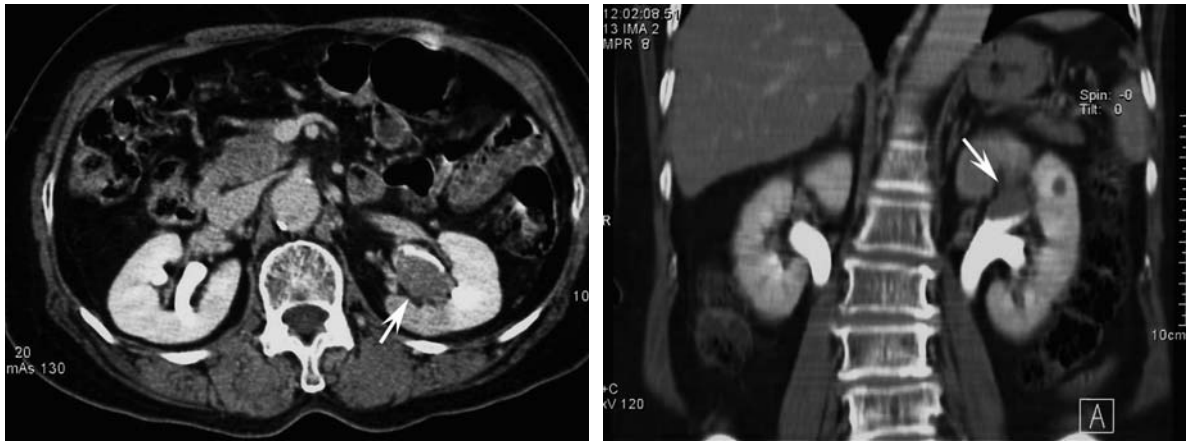

a **b**

Fig. 12.6a,b. Transitional cell carcinoma of the renal pelvis in a 73-year-old woman with a 1-month history of left flank pain and intermittent gross hematuria. **a** Axial contrast-enhanced CT scan shows an ill-defined low-density mass lesion (*arrow*) in the renal pelvis of the left kidney. **b** Coronal reformatted contrast-enhanced CT scan obtained during the excretory phase shows the tumor involvement of the renal pelvis and upper calyces (*arrow*) and clearly demonstrates the extent of this renal pelvis tumor. Note that the renal sinus fat is not obliterated and the renal contour is preserved. On pathologic examination, papillary transitional cell carcinoma was found in the renal pelvis and upper-pole calyx without invasion into the renal parenchyma.

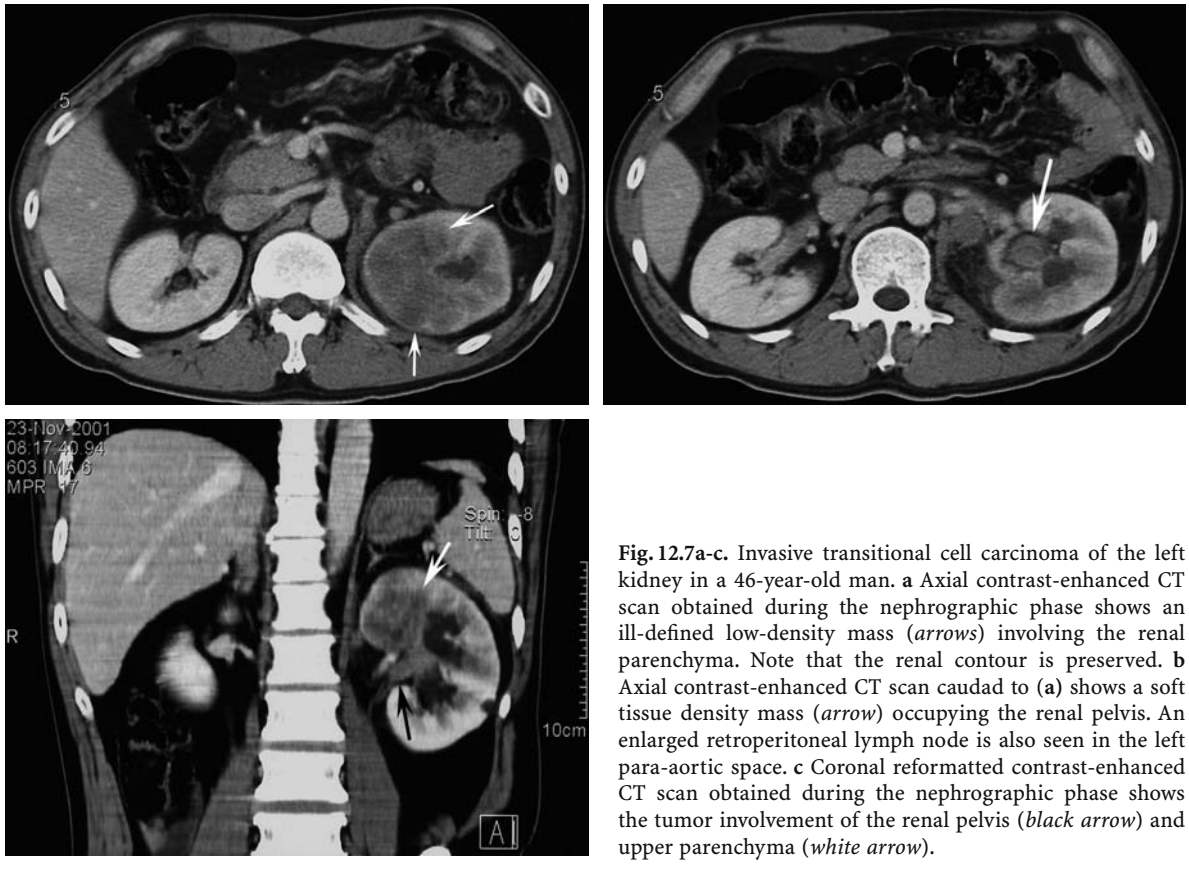

a **b** **c**

Fig. 12.7a-c. Invasive transitional cell carcinoma of the left kidney in a 46-year-old man. **a** Axial contrast-enhanced CT scan obtained during the nephrographic phase shows an ill-defined low-density mass (*arrows*) involving the renal parenchyma. Note that the renal contour is preserved. **b** Axial contrast-enhanced CT scan caudad to **(a)** shows a soft tissue density mass (*arrow*) occupying the renal pelvis. An enlarged retroperitoneal lymph node is also seen in the left para-aortic space. **c** Coronal reformatted contrast-enhanced CT scan obtained during the nephrographic phase shows the tumor involvement of the renal pelvis (*black arrow*) and upper parenchyma (*white arrow*).

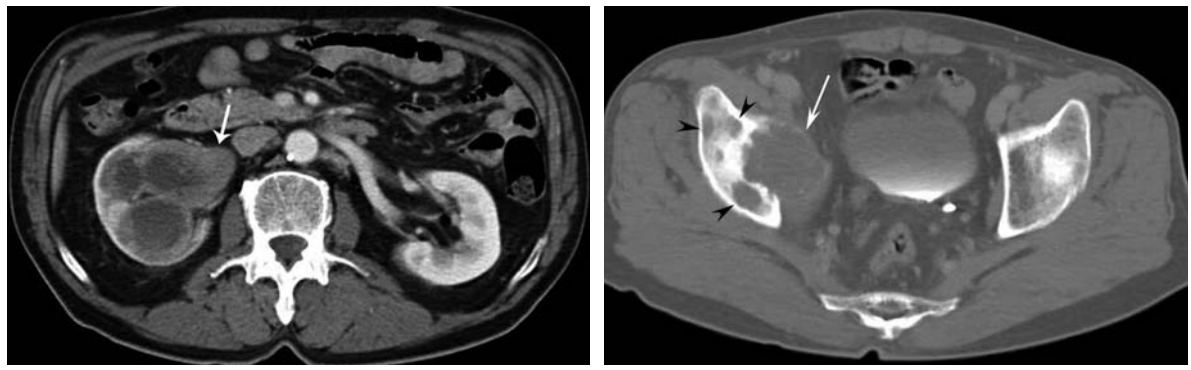

Fig. 12.8a,b. Invasive transitional cell carcinoma with bone metastasis in a 64-year-old man. **a** Axial contrast-enhanced CT scan obtained during the nephrographic phase shows an ill-defined hypodense tumor (*arrow*) in the dilated renal pelvis growing into the renal parenchyma while preserving the reniform outline of the right kidney. **b** Axial CT scan at the level of the sacrum shows a large expansile mass (*arrow*) with multifocal bone destruction in the right iliac bone (*arrowheads*).

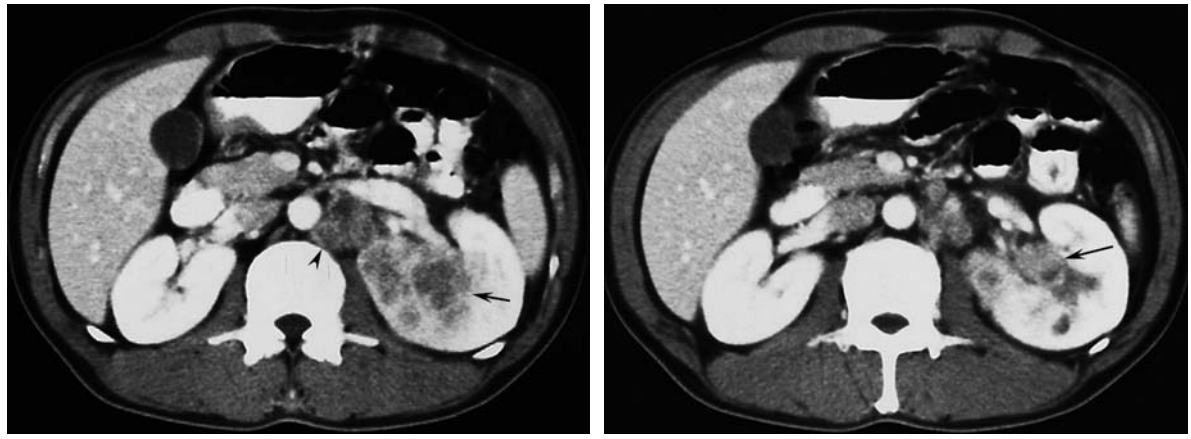

Fig. 12.9a,b. Squamous cell carcinoma in a 57-year-old man. **a** Axial contrast-enhanced CT scan obtained during the nephrographic phase shows centrally located ill-defined tumor (*arrow*) in the left kidney and left para-aortic lymphadenopathy (*arrowhead*). **b** Axial contrast-enhanced CT scan 1 cm caudad to (**a**) shows tumor infiltrating into the renal sinus (*arrow*). This tumor cannot be differentiated from transitional cell carcinoma by this CT finding.

12.4 Mesenchymal Tumors of the Renal Sinus

Primary mesenchymal origin tumors of the kidney are rare but may develop in the renal sinus space as well as in the renal capsule and renal parenchyma. The malignant renal neoplasms of pure mesenchymal origin are leiomyosarcoma, fibrosarcoma, liposarcoma, hemangiopericytoma, malignant fibrous histiocytoma, etc. (Choi et al. 1996; Shirkhoda and Lewis 1987). Leiomyosarcoma is the most common malignant tumor of primary mesenchymal origin neoplasms (Shirkhoda and Lewis 1987). The previously reported benign tumors should be known for their differential diagnosis purpose and include hemangioma, fibroma, leiomyoma, angiomyolipoma, neurogenic tumor, teratoma, etc. (Borrego et al. 1995; Cormier et al. 1989; Dasgupta et al. 1998; Ewald et al. 1982; Lee et al. 2000; Metro et al. 2000; Yoon et al. 1997; Yusim et al. 2001; Walther 1997).

Imaging findings of these rare tumors are usually nonspecific; however, the common imaging findings of primary mesenchymal origin tumors of the renal sinus are that the mass is relatively well circumscribed, the epicenter of the mass is located at the renal sinus, the mass is surrounded by attenuated renal parenchyma, and the renal pelvis is stretched over the tumor with or without hydronephrosis. It is important to make an accurate preoperative diagnosis of benign mesenchymal tumor because the treatment of choice is surgical or endoscopic excision,

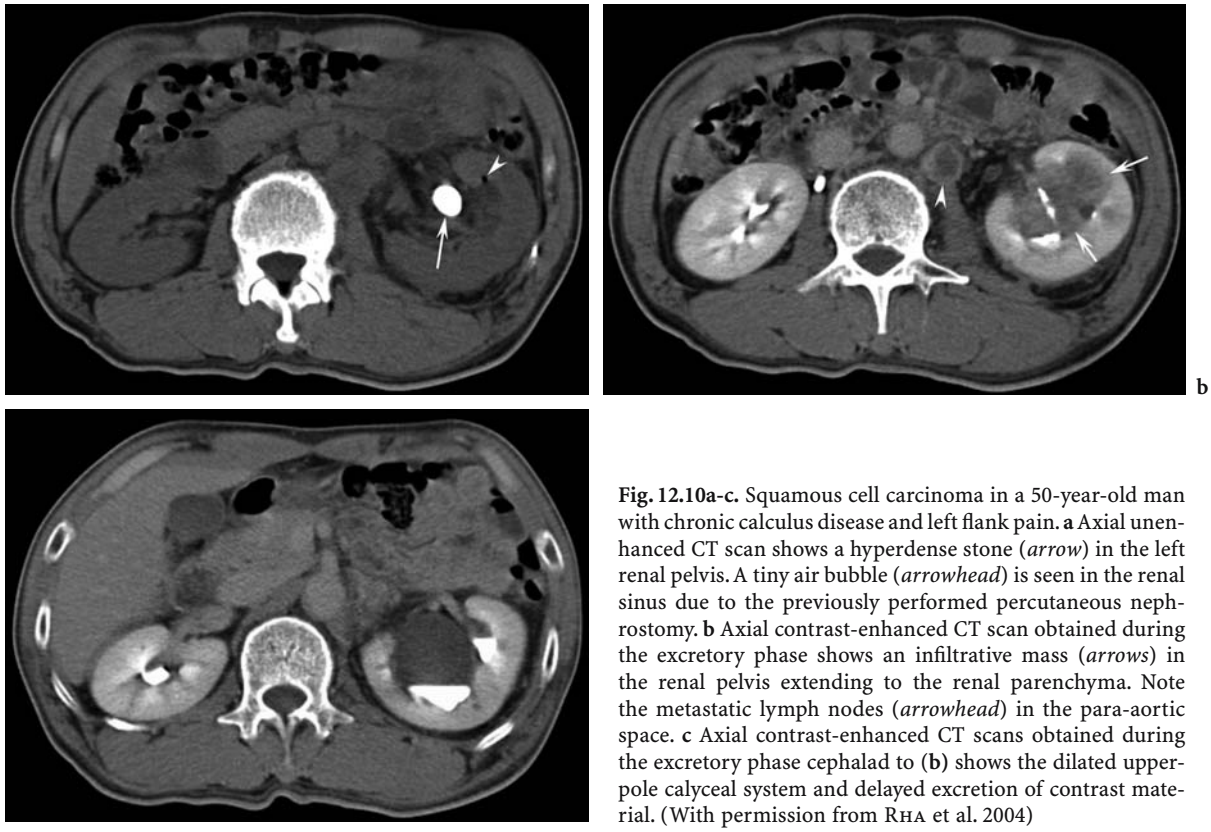

Fig. 12.10a-c. Squamous cell carcinoma in a 50-year-old man with chronic calculus disease and left flank pain. **a** Axial unenhanced CT scan shows a hyperdense stone (*arrow*) in the left renal pelvis. A tiny air bubble (*arrowhead*) is seen in the renal sinus due to the previously performed percutaneous nephrostomy. **b** Axial contrast-enhanced CT scan obtained during the excretory phase shows an infiltrative mass (*arrows*) in the renal pelvis extending to the renal parenchyma. Note the metastatic lymph nodes (*arrowhead*) in the para-aortic space. **c** Axial contrast-enhanced CT scans obtained during the excretory phase cephalad to (**b**) shows the dilated upper-pole calyceal system and delayed excretion of contrast material. (With permission from Rha et al. 2004)

but a preoperative differential diagnosis is difficult to make and these kinds of tumors are usually misdiagnosed preoperatively as the more common renal cell carcinomas or transitional cell carcinomas and are consequently treated with nephroureterectomy or radical nephrectomy, even in the benign cases (Yusim et al. 2001).

12.4.1 Leiomyosarcoma

Leiomyosarcoma of kidney, although a rare neoplasm, represents 2–3% of all malignant renal tumors. The origin of the renal leiomyosarcoma is generally from the interlacing bundles of smooth muscle in the inner layer of the renal capsule, in the wall of the renal pelvis, and within vessels of the renal parenchyma. About 33–58% of renal sarcomas are leiomyosarcoma (Shirkhoda and Lewis 1987). When the leiomyosarcoma is located within the renal parenchyma, it is difficult to differentiate from renal cell carcinoma. Conversely, in the case of the renal sarcoma originating within the renal sinus, the renal parenchyma appears draped over the tumor. If a huge, well-encapsulated neoplasm originates from the renal sinus, the diagnosis of renal sarcoma should be considered (Fig. 12.11). Renal sarcoma generally has a poor prognosis and requires aggressive therapy, usually with radical nephrectomy and chemotherapy (Davis et al. 1992). The lungs are the most frequent site of metastases.

12.4.2 Hemangiopericytoma

Hemangiopericytoma is an uncommon neoplasm that can occur in the kidney as well as in several other organs. Only 22 cases of renal hemangiopericytoma have ever been reported. Affected patients range in age from 18 to 68 years (mean age 42 years). Pathologically, hemangiopericytoma arises from the renal capsule as well as from renal parenchyma. Only one case of hemangiopericytoma occurring in the renal sinus has been reported (Fig. 12.12; Choi et al. 1996). The prognosis of renal hemangiopericytoma is generally poor, with an overall mortality rate of 50% (Heppe et al. 1991).

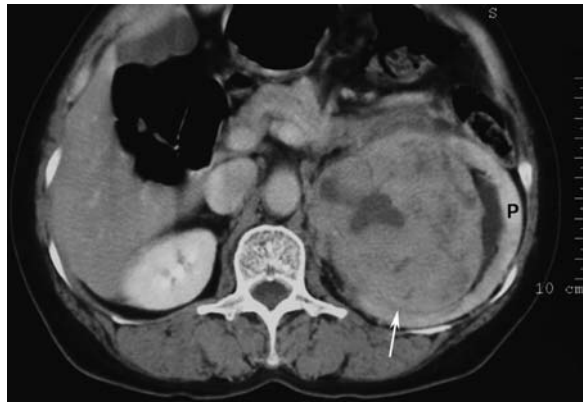

a

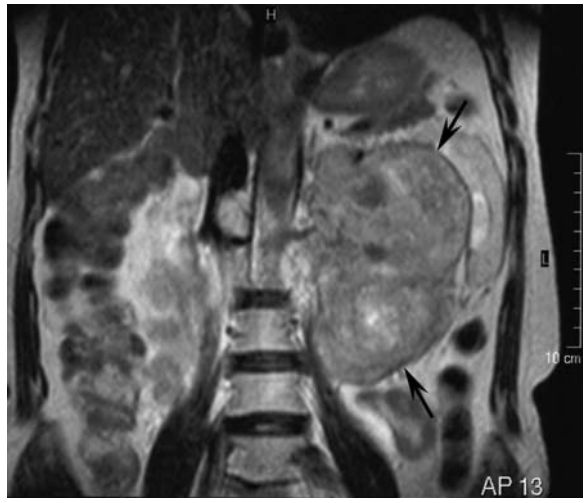

b

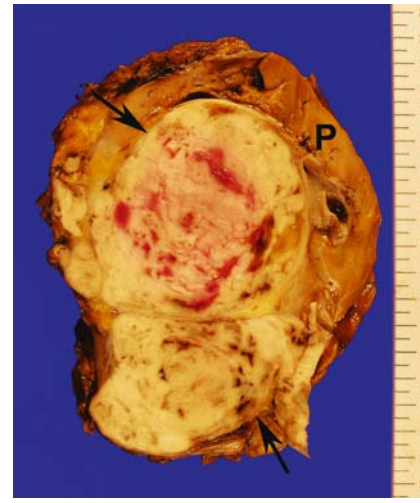

c

Fig. 12.11a-c. Leiomyosarcoma in the left renal sinus in a 65-year-old woman with left flank pain and a palpable left abdominal mass. **a** Axial contrast-enhanced CT scan shows a large heterogeneous-density mass (*arrow*) expanding the left renal sinus. The renal parenchyma *(P)* is markedly compressed and displaced laterally. **b** Coronal turbo spin-echo T2-weighted MR image (TR=6500 ms, TE=120 ms) clearly demonstrates the location and extent of the tumor (*arrows*). **c** Photograph of the surgical specimen shows a relatively well-defined tumor mass (*arrows*), 13×9×8 cm in size, located at the renal sinus. The mass shows a solid and compact cut surface with central hemorrhage and necrosis. The mass is confined to the sinus and does not invade the renal parenchyma or the pelvis. The adjacent renal parenchyma *(P)* is compressed by the tumor mass. (With permission from Rha et al. 2004)

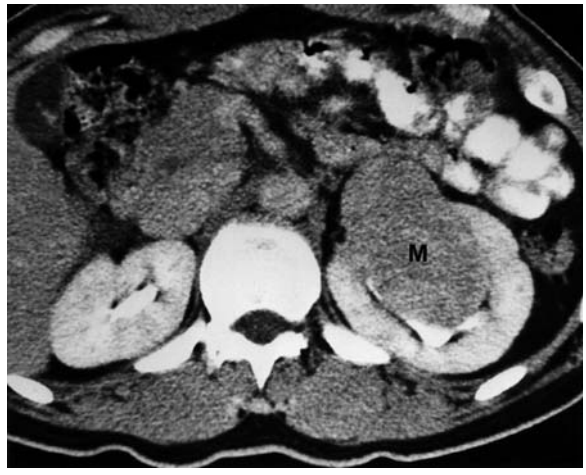

Fig. 12.12. Hemangiopericytoma in the left renal sinus in a 30-year-old woman with generalized weakness. Axial contrast-enhanced CT scan shows a large, well-defined, soft-tissue-density mass *(M)* occupying the central portion of the left renal sinus and compressing the opacified pelvocalyceal systems. (With permission from Rha et al. 2004)

12.4.3 Differential Diagnosis

It is essential to determine preoperatively the differential diagnosis of a variety of mesenchymal tumors, especially the benign tumors. Although this can be difficult, every effort should be made to arrive at the correct diagnosis.

Although renal hemangioma can be found in any part of the kidney, it usually occurs in the mucosa or subepithelial tissue of the pelvis (48.7%), in the pyramid (42.1%), and in the cortex of the kidney (9.2%; Virgili 2003). It is one of the benign causes of hematuria in young adults. Renal pelvis hemangiomas vary in size from microscopic to 10 cm or more but usually measure 1–2 cm. There are no specific clinical or radiologic findings for hemangiomas. Interestingly, even though this mass is a vascular tumor, the hemangioma may not enhance on contrast-enhanced CT scans depending on intratumoral hemorrhage or thrombosis of the vessels perfusing the mass. Renal hemangioma should be

included in the differential diagnosis, especially when CT shows little enhancement of the renal mass located at the pelvocalyceal junction or in the inner medulla (Fig. 12.13; Lee et al. 2000).

Renal leiomyoma is an uncommon benign tumor but is the most common among benign mesothelial tumors encountered in the genitourinary tract with an incidence of about 5% at autopsy (Yusim et al. 2001). It originates from the smooth muscle found in the renal capsule, renal pelvis, and vasculature. Computed tomography findings are variable from purely cystic to entirely solid lesions depending on their variable consistency (Fig. 12.14; Dasgupta 1998).

12.5 Renal Parenchymal Tumors Projecting into the Renal Sinus

Most renal parenchymal tumors grow by expansion, manifesting as ball-like masses (Zagoria and Tung 1997a). The medially growing renal parenchymal mass may project into the renal sinus and compress or infiltrate the renal sinus fat. The representative tumors are renal cell carcinoma and benign multilocular cystic nephroma.

12.5.1 Renal Cell Carcinoma

Renal cell carcinomas are the most common malignant renal parenchymal neoplasms. Most renal cell carcinomas grow by expansion and commonly extend into the renal sinus, leading to focal hydronephrosis or calyceal displacement (Figs. 12.15, 12.16; Zagoria and Tung 1997a). The clinical significance of renal cell carcinoma extending into the renal sinus is that the imaging appearance may be similar to that of transitional cell carcinoma, and tumor staging influences surgical management. Unlike transitional cell carcinoma, renal cell carcinoma has a tendency to extend into the venous system (Fig. 12.17). Although indications for partial nephrectomy are constantly changing, the most suitable indication for partial nephrectomy is a renal tumor smaller than 3 cm without invasion of the renal sinus fat, perinephric fat, or renal collecting system, particularly in patients with diminished renal function, and a solitary kidney or bilateral renal malignancy (Pretorius et al. 1999). Invasion of renal sinus fat indicates that partial nephrectomy cannot successfully and completely remove the renal mass. Three-dimensional CT or MR imaging helps to delineate the precise location of the renal mass and its relationship to the collecting system and renal vessels.

12.5.2 Multilocular Cystic Nephroma

Multilocular cystic nephromas are benign multiseptated cystic tumors originating from the renal parenchyma. These tumors have a biphasic age distribution, occurring predominantly in boys and middle-aged women. The gross finding of multilocular cystic nephroma is a solitary, well-

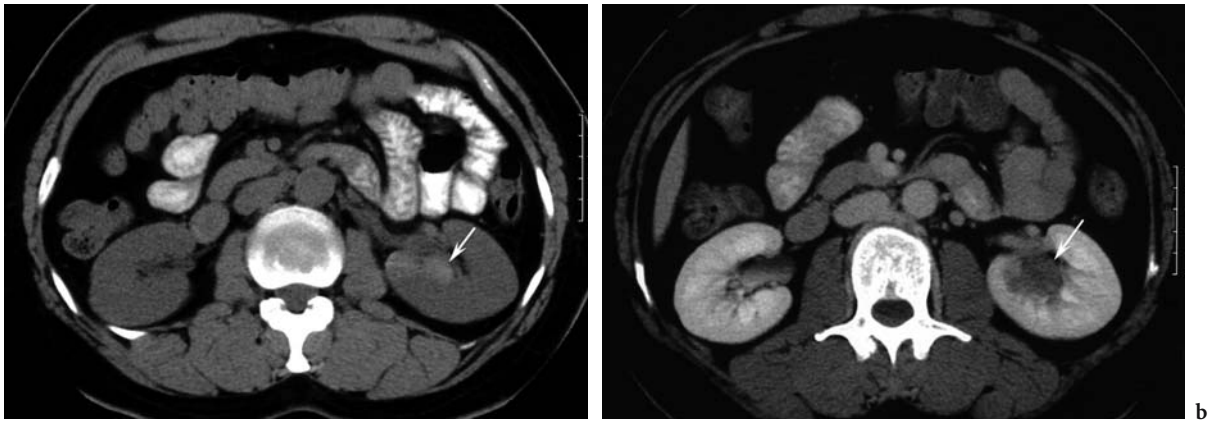

Fig. 12.13a,b. Venous hemangioma in the left renal sinus in a 33-year-old man with gross hematuria and left flank pain. **a** Axial unenhanced CT scan shows a well-defined hyperdense lesion (*arrow*) adjacent to the left renal pelvis. **b** Axial contrast-enhanced CT scan shows a poorly enhancing, hypodense mass (*arrow*). Because of the possibility of malignancy, a left nephrectomy was performed. At pathologic examination, the lesion was composed of multiple vascular channels of variable sizes beneath the pelvic mucosa. (With permission from Rha et al. 2004)

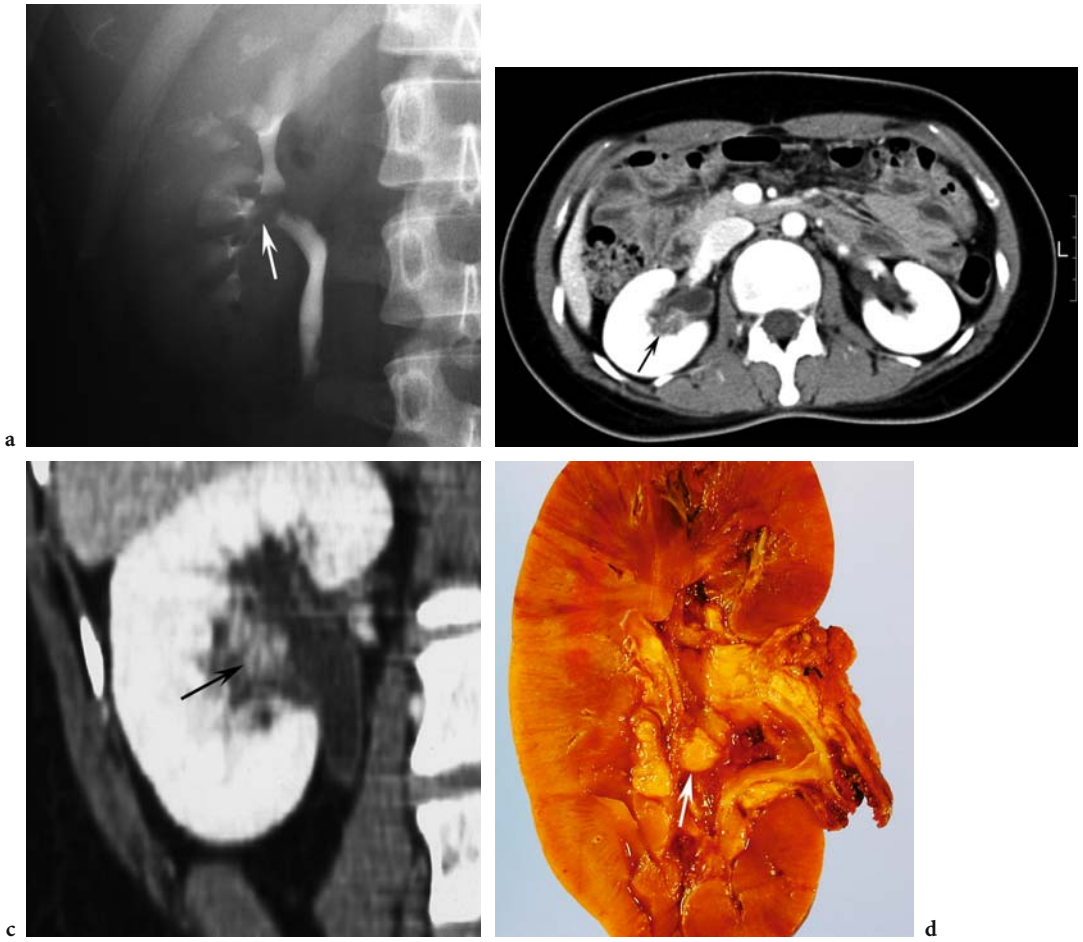

Fig. 12.14a-d. Leiomyoma involving the renal sinus in a 28-year-old woman with gross hematuria. **a** Excretory urography shows a focal smooth mass effect on the pelvocalyces of the right kidney (*arrow*). **b** Axial contrast-enhanced CT scan obtained during the nephrographic phase shows a small soft-tissue-density mass (*arrow*) obliterating the sinus fat in the right kidney along the posterior margin of the right renal pelvis. **c** Coronal reformatted CT scan demonstrates a round soft-tissue-density mass lesion (*arrow*) in the right renal sinus and mild dilation of the pelvocalyceal system. **d** Photograph of the surgical specimen shows a well-defined round mass (*arrow*) in the renal sinus. Microscopic examination reveals a renal leiomyoma in the right renal sinus. (With permission from Rha et al. 2004)

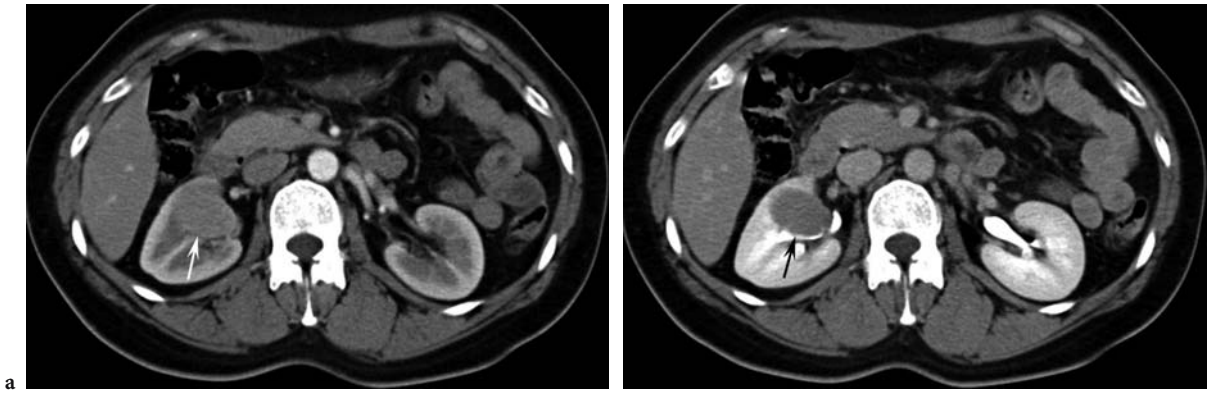

Fig. 12.15a,b. Renal cell carcinoma located near the renal sinus in a 43-year-old woman. **a** Axial contrast-enhanced CT scan obtained during the corticomedullary phase shows a large, well-defined, soft-tissue-density mass (*arrow*) in the central portion of the right kidney. **b** Axial contrast-enhanced CT scan obtained during the excretory phase shows the mass indenting the opacified pelvocalyceal systems (*arrow*). Pathology confirmed chromophobe-type renal cell carcinoma near the renal sinus without invasion of the renal vein or renal pelvis.

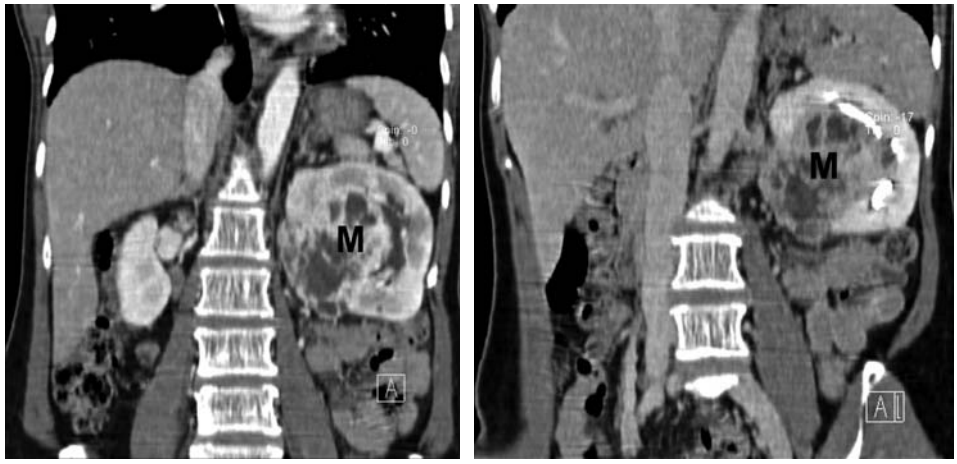

a b

Fig. 12.16a,b. Centrally located renal cell carcinoma in a 56-year-old woman. Coronal reformatted contrast-enhanced CT scans obtained during **a** the corticomedullary phase and **b** the excretory phase show a large lobulated heterogeneous density mass *(M)* involving the left renal sinus.

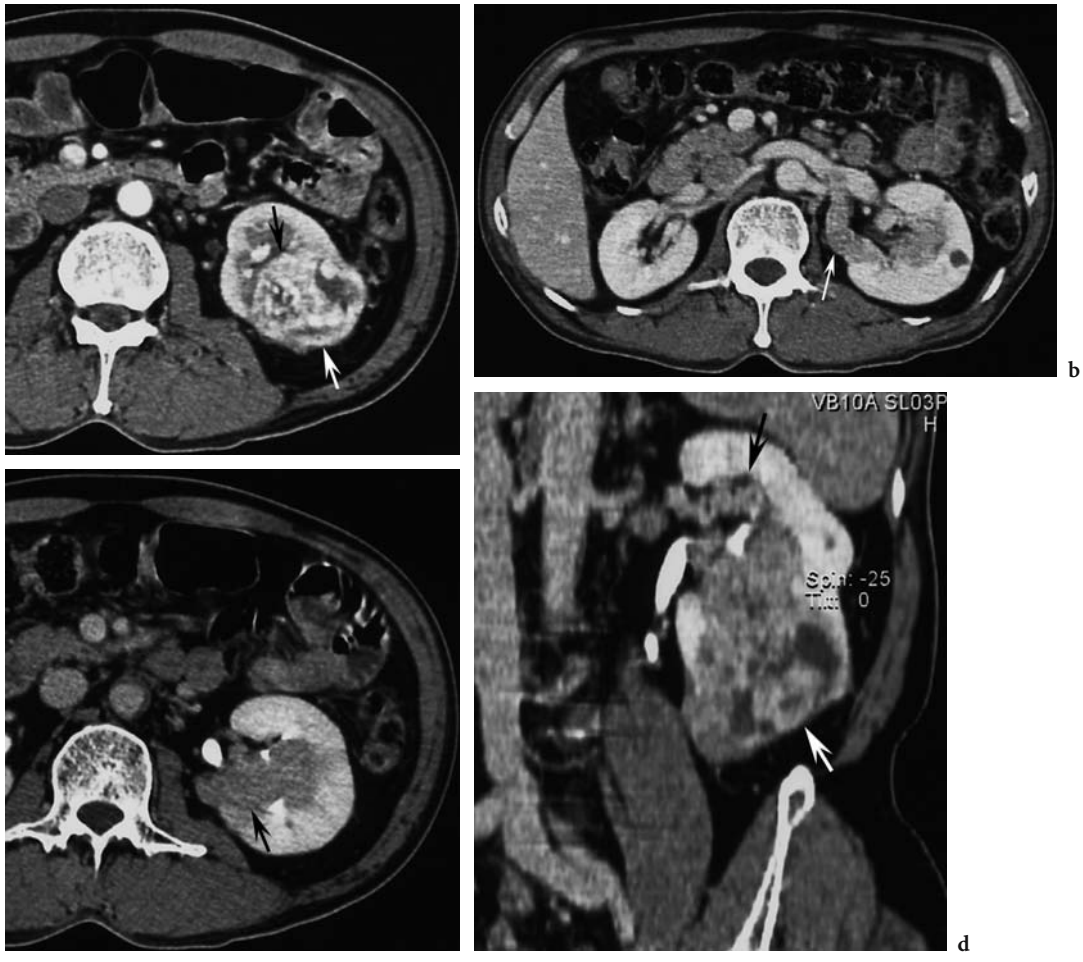

a b c d

Fig. 12.17a-d. Renal cell carcinoma extension into the renal sinus in a 51-year-old man with gross hematuria. **a** Axial contrast-enhanced CT scan shows a lobulated heterogeneously enhancing tumor (*arrows*) involving the lower pole of the left kidney. **b** Axial contrast-enhanced CT scan obtained 1 cm cephalad to **a** shows the posterior segmental branch of the left renal vein occupied by the tumor thrombus (*arrow*). **c** Axial contrast-enhanced CT scan obtained 2 cm cephalad to **a** shows the tumor extending to the left renal sinus (*arrow*). **d** Coronal reformatted contrast-enhanced CT obtained during the excretory phase clearly shows the tumor involvement of the renal sinus and the extent of the renal cell carcinoma (*arrows*). These findings were confirmed at radical nephrectomy. The pathologic stage was T3b N0. (With permission from Rha et al. 2004)

circumscribed, multiseptated mass of noncommunicating fluid-filled loculi, surrounded by a thick fibrous capsule and compressed renal parenchyma (Madewell et al. 1983). Interestingly, this lesion frequently herniates into the renal sinus, causing a filling defect in the renal pelvis and sometimes obstructive caliectasia (Madewell et al. 1983), but this sign is nonspecific and may be present in case of Wilms tumor or renal cell carcinoma. On imaging studies, multilocular cystic nephroma presents as a well-defined encapsulated cystic mass containing numerous thick septa (Fig. 12.18; Zagoria and Tung 1997b). Although the typical findings are present, the possibility of cystic renal cell carcinoma or Wilms' tumor cannot be entirely excluded; therefore, surgery is indicated, even when the diagnosis of multilocular cystic nephroma is strongly suspected (Castillo et al. 1991).

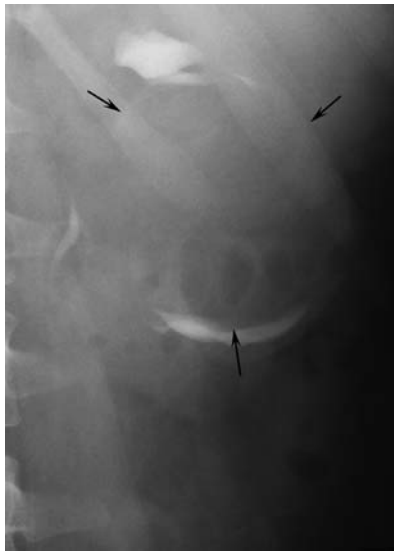

a

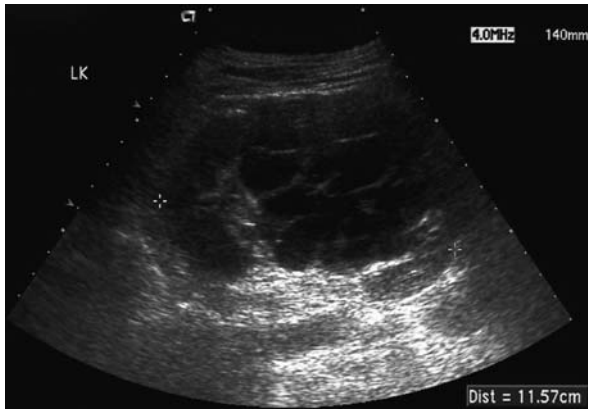

b

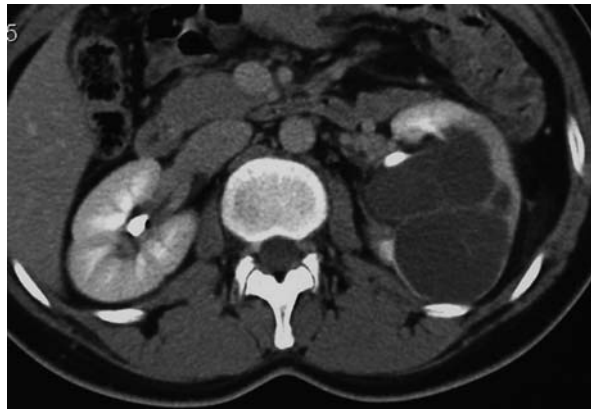

c

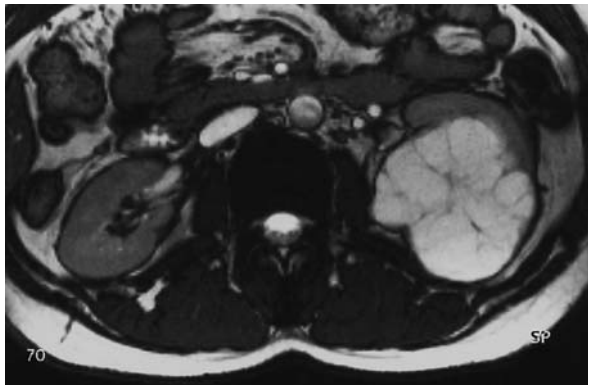

d

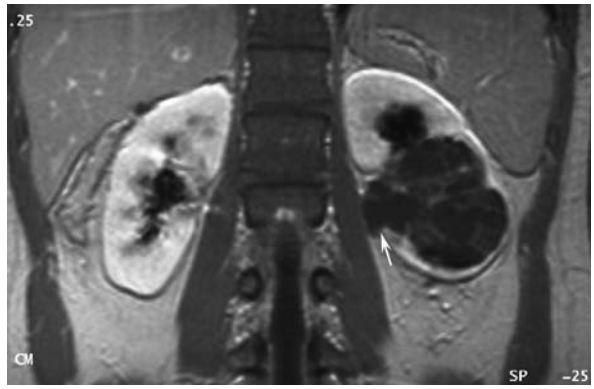

e

Fig. 12.18a-e. Multilocular cystic nephroma in a 32-year-old man. **a** Excretory urography shows marked splaying of the upper and lower calyceal systems (*arrows*) with mild dilation of the upper pole calyx. **b** Longitudinal US image of the left kidney shows a multiloculated cystic mass in the lower pole of the left kidney. **c** Axial contrast-enhanced CT scan obtained during the excretory phase shows a well-defined multi-chambered cystic mass in the left kidney. **d** Axial true fast imaging with steady-state precession MR image (TR=6.3 ms, TE=3.0 ms, flip angle 70°) again shows a hyperintense cystic mass in the left kidney. Note the numerous fine septations without solid components. **e** Coronal contrast-enhanced T1-weighted MR image (TE=130 ms, TE=4.1 ms) clearly shows herniation of the cystic mass (*arrow*) into the renal sinus. (With permission from Rha et al. 2004)

12.6 Retroperitoneal Tumors Extending to the Renal Sinus

12.6.1 Lymphoma

As the renal sinus is a medial extension of the perinephric space, any retroperitoneal tumor can extend to the renal sinus (Fig. 12.19). The representative example is a lymphoma. Retroperitoneal lymphoma with contiguous extension into the renal sinus is a common manifestations of lymphoma (Urban and Fishman 2000). These patients present with a large, bulky retroperitoneal mass that envelops and surrounds the normal constituents of the renal sinus, often with contiguous spread into the perinephric space (Fig. 12.20). This situation is most common in patients with advanced non-Hodgkin lymphoma. The renal vessels remain patent despite tumor encasement, a finding that is characteristic for lymphoma. Conversely, obstructive hydronephrosis is often caused by direct involvement of the renal collecting system (Jafri et al. 1982; Urban and Fishman 2000). Renal lymphoma can also infiltrate the renal sinus or the renal parenchyma, maintaining its reniform shape (Fig. 12.21). On CT and US, lymphomatous masses are characteristically homogeneous. On CT, the mass enhances less. Renal lymphoma is usually hypoechoic on US, a finding that reflects tissue homogeneity. On MR imaging, renal lymphoma tends to be hypointense relative to the renal cortex on T1-weighted images and hetero-

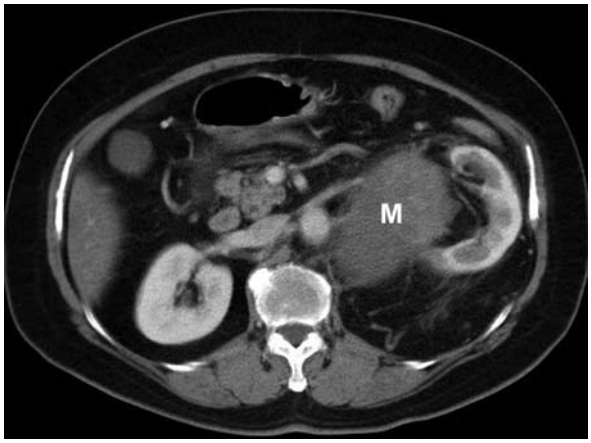

a

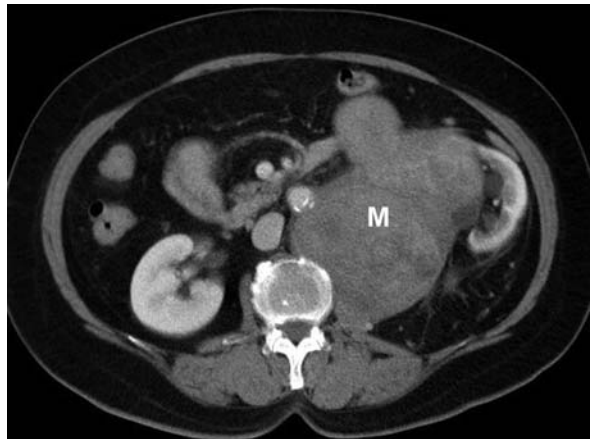

b

Fig. 12.19a,b. Retroperitoneal spindle cell tumor extending to the renal sinus in a 63-year-old woman. **a, b** Axial contrast-enhanced CT scans show a bulky lobulated soft-tissue-density mass *(M)* in the left para-aortic space and extending to the left renal sinus. It causes dilation of the left renal pelvis and calyces.

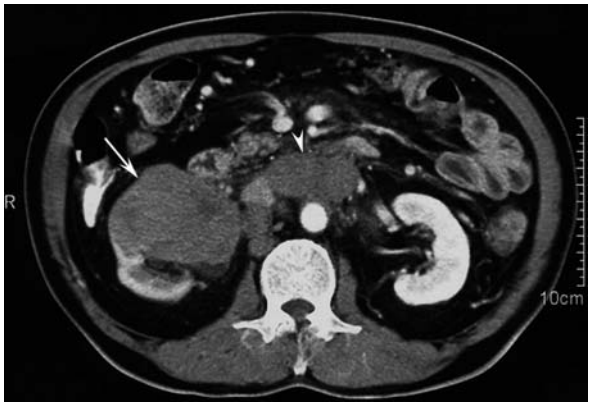

a

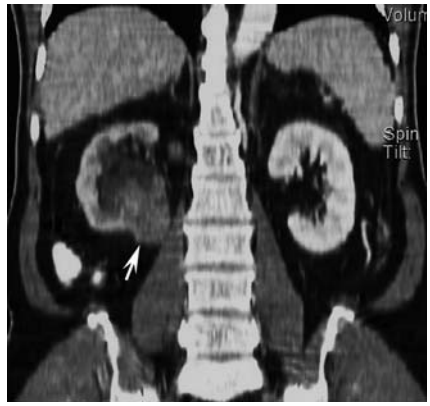

b

Fig. 12.20a,b. Lymphoma involving the renal parenchyma and renal sinus in a 56-year-old man with generalized weakness. **a** Axial contrast-enhanced CT scan shows a large relatively homogeneous mass (*arrow*) involving the right renal parenchyma and renal sinus. Note the multiple enlarged retroperitoneal lymph nodes (*arrowhead*). **b** Coronal reformatted CT scan obtained during the nephrographic phase shows the extent of the lymphoma mass (*arrow*) and mild hydronephrosis of the right kidney. (With permission from Rha et al. 2004)

geneously hypointense or isointense on T2-weighted images. Minimal enhancement is generally detected, although renal lymphoma enhances considerably less than normal renal parenchyma.

12.6.2 Metastasis

Metastasis to the sinus lymph nodes occurs either as part of a generalized retroperitoneal process or as an isolated involvement, as with primary gonadal tumors, because of rich supply of perforating capsular vessels and lymphatics into the renal sinus (Fig. 12.22; Davidson et al. 1999).

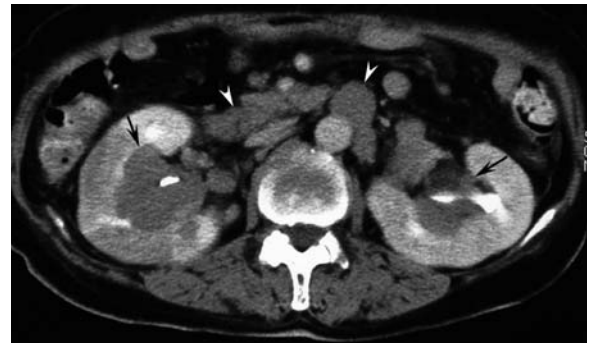

Fig. 12.21. Peripelvic lymphoma in a 63-year-old woman. Axial contrast-enhanced CT scan shows soft tissue density masses involving the renal sinus of both kidneys (*arrows*). Multiple retroperitoneal lymph nodes (*arrowheads*) are also seen.

12.7 Conclusion

A broad pathologic spectrum of tumors can occur in the renal sinus. The diagnosis and exact preoperative staging of renal sinus tumors relies on a multimodality imaging approach that includes excretory urography, US, CT, MR imaging, and angiography. Ultrasound is an excellent noninvasive technique to confirm whether such a mass is cystic or solid. If US findings suggest a solid mass, CT or MR imaging is used as a problem-solving technique and for evaluation of the staging or to determine the extent of the lesion. In general, the coronal plane of cross-sectional imaging is the most useful for the evaluation of renal sinus lesions, because it provides a comprehensive view of complicated renal sinus pathology. Familiarity with the imaging features and differential diagnoses of various renal sinus tumors will facilitate prompt, accurate diagnosis and treatment.

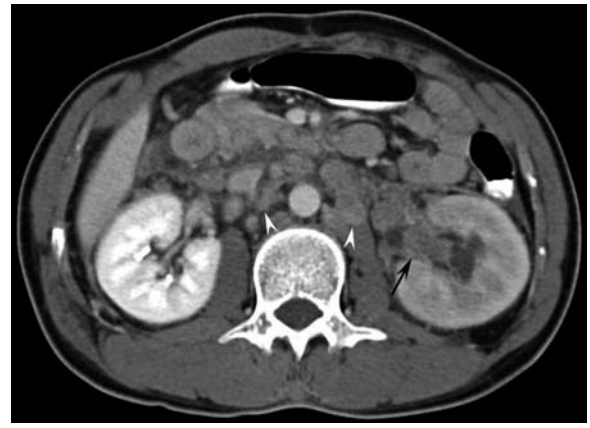

Fig. 12.22. Metastatic lymphadenopathy from ascending colon cancer involving the left renal sinus in a 36-year-old man. Axial contrast-enhanced CT scan shows multiple soft-tissue-density lymph nodes (*arrowheads*) in the retroperitoneum extending to the left renal sinus (*arrow*) with mild obstructive hydronephrosis of the left kidney.

References

Amis ES Jr (2000) Cysts of the renal sinus. In: Pollack HM, McClennan BL (eds) Clinical urography, 2nd edn. Saunders, Philadelphia, pp 1404–1412

Amis ES Jr, Cronan JJ (1988) The renal sinus: an imaging review and proposed nomenclature for sinus cysts. J Urol 139:1151–1159

Baron RL, McClennan BL, Lee JK et al. (1982) Computed tomography of transitional cell carcinoma of the renal pelvis and ureter. Radiology 144:125–130

Blacher EJ, Johnson DE, Abdul-Karim FW et al. (1985) Squamous cell carcinoma of renal pelvis. Urology 25:124–126

Bonsib SM, Gibson D, Mhoon M, Greene GF (2000) Renal sinus involvement in renal cell carcinomas. Am J Surg Pathol 24:451–458

Borrego J, Cuesta C, Allona A et al. (1995) Myxoid neurofibroma of the renal sinus. Actas Urol Esp 19:415–418

Castillo OA, Boyle ET Jr, Kramer SA (1991) Multilocular cysts of kidney: a study of 29 patients and review of literature. Urology 37:156–162

Choi YJ, Hwang TK, Kang SJ et al. (1996) Hemangiopericytoma of renal sinus expanding to the renal hilum: an unusual presentation causes misinterpretation as transitional cell carcinoma. J Korean Med Sci 11:351–355

Cormier P, Patel SK, Turner DA et al. (1989) MR imaging

findings in renal medullary fibroma. Am J Roentgenol 153:83–84
Dasgupta P, Sandison A, Parks C et al. (1998) Case report: Renal leiomyoma with unusual calcification. Clin Radiol 53:857–858
Davidson AJ, Hartman DS, Choyke PL et al. (1999) Renal sinus and periureteral abnormalities. In: Davidson AJ, Hartman DS, Choyke PL et al. (eds) Davidson's radiology of the kidney and genitourinary tract, 3rd edn. Saunders, Philadelphia, pp 431–455
Davis R, Vaccaro JA, Hodges GF (1992) Renal leiomyosarcoma: plea for aggressive therapy. Urology 40:168–171
Ewald N, Cukier J, Roth A et al. (1982) Teratoma of the renal sinus. Apropos of a case. J Urol (Paris) 88:553–554
Heppe RK, Donohue RE, Clark JE (1991) Bilateral renal hemangiopericytoma. Urology 38:249–253
Jafri SZ, Bree RL, Amendola MA et al. (1982) CT of renal and perirenal non-Hodgkin lymphoma. Am J Roentgenol 138:1101–1105
Jeffrey RB Jr (2004) Clinical impact of multidetector CT. In: Fishman EK, Jeffrey RB Jr (eds) Multidetector CT. Principles, techniques, and clinical applications. Lippincott Williams and Wilkins, Philadelphia, pp 53–58
Kawashima A, Goldman SM (2000) Neoplasms of the renal collecting system, pelvis, and ureters. In: Pollack HM, McClennan BL (eds) Clinical urography, 2nd edn. Saunders, Philadelphia, pp 1560–1641
McLaughlin JK, Blot WJ, Mandel JS et al. (1983) Etiology of cancer of the renal pelvis. J Natl Cancer Inst 71:287–291
Lee HS, Koh BH, Kim JW et al. (2000) Radiologic findings of renal hemangioma: report of three cases. Korean J Radiol 1:60–63
Madewell JE, Goldman SM, Davis CJ Jr et al. (1983) Multilocular cystic nephroma: a radiographic–pathologic correlation of 58 patients. Radiology 146:309–321
Metro MJ, Ramchandani P, Banner MP et al. (2000) Angiomyolipoma of the renal sinus: diagnosis by percutaneous biopsy. Urology 55:286
Narumi Y, Sato T, Hori S et al. (1989) Squmous cell carcinoma of the uroepithelium: CT evaluation. Radiology 173:853–856
Pickhardt PJ, Lonergan GJ, Davis CJ Jr et al. (2000) Infiltrative renal lesions: radiologic–pathologic correlation. Radiographics 20:215–243
Pozzi-Mucelli R, Rimondini A, Morra A (2004) Radiologic evaluation in planning surgery of renal tumors. Abdom Imaging 29:312–319
Pretorius ES, Siegelman ES, Ramchandani P et al. (1999) Renal neoplasms amenable to partial nephrectomy: MR imaging. Radiology 212:28–34
Rha SE, Byun JY, Jung SE et al. (2004) The renal sinus: pathologic spectrum and multi-modality imaging approach. Radiographics 24 (Suppl 1):S117–S131
Rosenfield AT, Taylor KJ, Dembner AG et al. (1979) Ultrasound of renal sinus: new observations. Am J Roentgenol 133: 441–448
Shirkhoda A, Lewis E (1987) Renal sarcoma and sarcomatoid renal cell carcinoma: CT and angiographic features. Radiology 162:353–357
Urban BA, Fishman EK (2000) Renal lymphoma: CT patterns with emphasis on helical CT. Radiographics 20:197–212
Urban BA, Buckley J, Soyer P et al. (1997) CT appearance of transitional cell carcinoma of the renal pelvis. Part 1. Early-stage disease. Am J Roentgenol 169:157–161
Urban BA, Buckley J, Soyer P et al. (1997) CT appearance of transitional cell carcinoma of the renal pelvis. Part 2. Advanced-stage disease. Am J Roentgenol 169:163–168
Virgili G, Stasi SM di, Bove P et al. (2003) Cavernous hemangioma of the renal hilum presenting as an avascularized solid mass. Urol Int 71:325–328
Walther PJ (1997) Uncommon neoplasms of the kidney. In: Raghavan D, Scher HI, Leibel SA, Lange PH (eds) Principles and practice of genitourinary oncology. Lippincott-Raven, Philadelphia, pp 897–909
Wimbish KJ, Sanders MM, Samuels BI et al. (1983) Squamous cell carcinoma of the renal pelvis: case report emphasizing sonographic and CT appearance. Urol Radiol 5:267–269
Wong-You-Cheong JJ, Wagner BJ, Davis CJ Jr (1998) Transitional cell carcinoma of the urinary tract: radiologic–pathologic correlation. Radiographics 18:123–142
Yoon YD, Byun JY, Jee WH et al. (1997) Imaging diagnosis in various renal sinus lesions. J Korean Radiol Soc 37:509–514
Yusim IE, Neulander EZ, Eidelberg I et al. (2001) Leiomyoma of the genitourinary tract. Scand J Urol Nephrol 35:295–299
Zagoria RJ, Tung GA (1997) Renal masses. In: Zagoria RJ, Tung GA (eds) Genitourinary radiology: the requisites. Mosby, St. Loius, pp 81–121
Zagoria RJ, Tung GA (1997) The renal sinus, pelvocalyceal system, and ureter. In: Zagoria RJ, Tung GA (eds) Genitourinary radiology: the requisites. Mosby, St. Louis, pp 152–191